

## Cluster model for compaction of vibrated granular materials

Konstantin L. Gavrilov\*

*Department of Physics and Enrico Fermi Institute, The University of Chicago, 5640 South Ellis Avenue, Chicago, Illinois 60637*

(Received 20 October 1997)

In this paper we present a one-dimensional model describing properties of compaction observed in recent experiments with vibrated granular materials. In this model, a granular material undergoing vertical vibrations is considered as a system of randomly packed clusters. Each cluster in the system is supposed to be hexagonally packed to the maximum possible density, and porosity of material arises from random packing of the clusters. Vibrations cause fragmentation of clusters through separation of individual particles from a cluster, and reassociation of the individual particles with surrounding clusters. This model successfully describes experimental results on the dynamics of granular compaction, reversible and irreversible behavior, dependence of the steady-state density on the magnitude of external vibrations, and predicts the crystallization of the material for a small magnitude of vibrations. It also connects microscopic properties of granular media with the experimental data on density fluctuations, such as temporal behavior, amplitude, and spectral properties of the fluctuations. In combination with experiment, this model can be instrumental in extracting constants of the mechanism and rate of cluster fragmentation, clusters arrangement in the media, and voids distribution. The importance and effectiveness of the cluster approach are discussed as the key points of the model. [S1063-651X(98)00908-8]

PACS number(s): 81.05.Rm, 05.40.+j, 46.10.+z

### I. INTRODUCTION

Settling of a vibrated granular material into a more compact state is important to a wide range of industries and in many technological processes in which the density of granular solids needs to be controlled [1]. The underlying structural and dynamic properties of granular systems are a subject of great interest for physicists [2–11]. To understand these properties, a number of studies in well controlled experimental conditions have been carried out [3,4]: monodisperse spherical glass particles were confined to a long, thin cylindrical tube and were subjected to vertical vibrations. The particles were baked prior to loading in the tube and maintained under vacuum to prevent uncontrollable cohesion between the particles and a change of their dielectric response due to the presence of water vapor. These experiments provided important information on time-dependent properties of compaction and were given a phenomenological description [5].

The theoretical understanding of compaction on a microscopic level is a nontrivial task, and still remains an open area of research [6–11]. We view an approach assuming two times of relaxation [4,7] for individual particles and for clusters of particles as an important step in the direction of creating a microscopic theory, because it connects the experimental phenomenological properties to the microstructure of granular media.

Clustering is a generic property of systems with dissipation [12,13] and can be a primary effect controlling the microdynamics of the systems through inelastic collapse [14–16] or through constraining the motion of individual particles in such systems [10]. Recently the cluster approach was used

successfully to explain nonlinear dynamic properties of uninterrupted traffic flow [17–19]. As will be shown here, the same approach can be successfully applied to interpret new results on the dynamics of compaction of granular material [20–22].

In the microscopic model that was developed, granular material undergoing vertical vibrations is considered as a system of randomly packed clusters that undergo fragmentation and reassociation. Motivation for its development and the underlying basic assumptions are described in Sec. II. In Sec. III, results of model simulations are presented, discussed, and compared with experiments. Discussed in Sec. IV is the microscopic basis of this model, and how it can be used in conjunction with experiment to study the microstructure and microdynamics of granular materials.

### II. DEVELOPMENT OF A MODEL OF GRANULAR COMPACTION

The starting point in the derivation of the model discussed here is the analogy in the structural and dynamic properties of a vibrated granular material with those of congested traffic flow.

The phenomenon of compaction results from the existence of packing defects, such as voids, in a randomly packed granular material [Fig. 1(a)]. Shaking of the material causes rearrangement of grains and voids. When a void becomes large enough in size to accommodate an overlaying grain, the grain falls into the void. Consecutive repetition of this process reduces porosity of the material and makes it denser.

Similar events occur in congested traffic flow, which is not perfectly homogeneous [19] [Fig. 1(b)], where car clusters are constantly involved in an aggregation-fragmentation process. In the description of the dynamics of traffic flow (in a regime less dense than that presented by gravitating granu-

---

\*FAX: (773) 702-8038. Electronic address: kgavrilov@rainbow.uchicago.edu

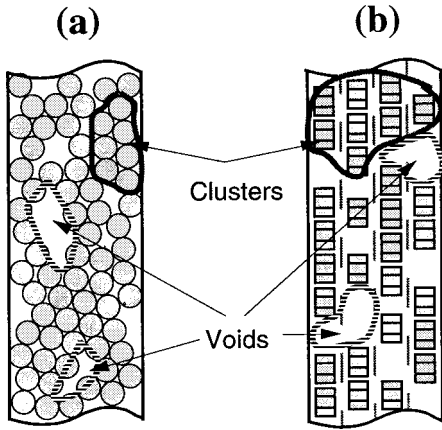


FIG. 1. Similarity between granular material and traffic flow: from structure to dynamics. (a) Graphical representation of granular material as a system of randomly packed clusters of particles with voids in between. Each cluster is packed to maximum possible density (hexagonal lattice). (b) Graphical representation of congested traffic flow as a system of randomly packed car clusters with voids between the clusters. Each car cluster is packed to its maximum possible density (“bumper-to-bumper”).

lar material), a cluster model was developed that was successful in explaining the nonlinear behavior of density fluctuations [17–19]. Because of the analogy, and earlier results on clustering in granular media [4,6,7,10–13], it is tempting to attempt a description of the latter media using an extension of the formalism that described the dynamics of traffic flow. For this task, the following assumptions were made about the structure and dynamics of a granular material.

#### A. Structure of a randomly packed granular material

(i) We consider a granular material undergoing vertical vibrations as a system of randomly packed clusters [Fig. 1(a)]. Each cluster in the system is supposed to be *ideally packed*, that is, to its maximum possible density. For a system of spherical beads, the maximum density is achieved by hexagonal packing and is equal to  $0.74\rho_0$ , where  $\rho_0$  is the density of the beads material.

(ii) The cluster view of granular media, (i), implies that the media can be subdivided into a number of subsystems (clusters), each ideally packed spontaneously. This gives rise to packing defects, voids, as a result of mismatched placing of the ideally packed clusters [Fig. 2(a)]. Then the volume of

voids introduced into the system by one cluster can be assumed to be proportional to the surface area of the cluster:

$$\Delta V_{\text{voids}} = v_1 j^{2/3}, \quad (1)$$

where  $j$  is the number of beads in the cluster and  $v_1$  is a coefficient of proportionality ( $v_1$  can be viewed as a mean void volume per one particle of a cluster surface).

Expression (1) makes porosity of granular media depend on the number and sizes of clusters in the media, i.e., the distribution of clusters,  $n_j$ , with respect to cluster size  $j$ . The total void volume can then be written as follows:

$$V_{\text{void total}} = v_1 \sum n_j j^{2/3}. \quad (2)$$

On this basis, a formula can be derived yielding the density  $\rho$  of a granular material consisting of  $N_{\text{tot}}$  beads, as a function of the cluster size distribution:

$$\rho = 0.74\rho_0 \frac{N_{\text{tot}} + v_1 N_{\text{tot}}^{2/3}}{N_{\text{tot}} + v_1 \sum_j n_j j^{2/3}}, \quad (3)$$

where  $N_{\text{tot}}$  is a total number of beads in the system. It is easy to see that, when all the  $N_{\text{tot}}$  beads are packed hexagonally into one cluster, expression (3) yields density  $0.74\rho_0$ .

One can also see a close resemblance between expression (3) and a phenomenological stroboscopic law, recently derived for compaction [5]. We consider this similarity as an important confirmation of the assumptions made about the microscopic structure and phenomenological behavior of granular materials.

#### B. Kinetics and dynamics of compaction: Shaking a system of clusters

We have assumed that vibrations cause fragmentation and reassociation of clusters.

(i) The fragmentation is considered as a process of separating individual particles from the cluster as a result of a sudden tap on the system.

Each tap would split a cluster  $c_j$  consisting of  $j$  particles into a cluster of  $(j-K)$  particles and  $K$  individual particles, if  $j > K$ , or just split the whole cluster into  $j$  individual particles, if  $j \leq K$ , where  $K$  is a model parameter, i.e.,

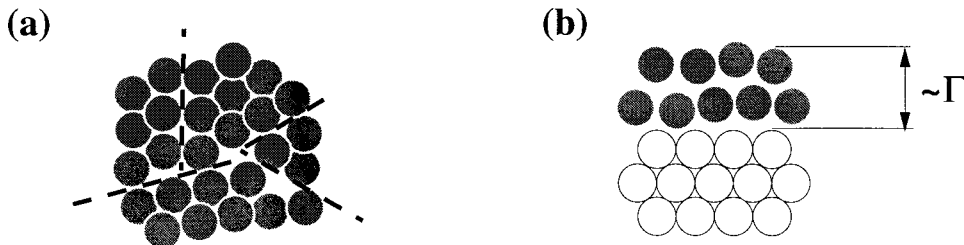


FIG. 2. (a) Demonstration of porosity of the granular material as a result of random packing of the clusters with hexagonal packing (described in Sec. II A). Areas of loose packing are indicated by dashed lines. (b) Graphical representation of the cluster fragmentation described in Sec. II B of the main text: The external tap on the system can lift beads. The larger the amplitude of the external force, the more beads become free and can take part in the fragmentation process, and, hence, the rate of clusters fragmentation is proportional to the dimensionless acceleration  $\Gamma$ .

$$c_j \rightarrow \begin{cases} c_{j-K} + Kc_1 & \text{if } j > K, \\ jc_1 & \text{if } j \leq K. \end{cases} \quad (4)$$

Expression (4) assumes that the fragmentation rate is independent of cluster size. We will discuss in Sec. IV how different fragmentation mechanisms with respect to cluster size  $j$  can influence the dynamic features of compaction.

The separation of a bead from a cluster is constrained by the particle's own weight as well as by the weights of other overlaying particles in the cluster. For this particle to separate from a cluster, it is necessary to overcome the constraining weight. The external tap on the system can relax this constraint by lifting the constraining weight. The larger the amplitude of the external force, the more particles become free and can take part in the fragmentation process [Fig. 2(b)]. For this reason, we assumed for the rate of cluster fragmentation a linear dependence on the shaking force, and, hence, the rate of clusters fragmentation is proportional to the "dimensionless acceleration"  $\Gamma$  ( $\Gamma = a_{\text{tap}}/g$ , where  $a_{\text{tap}}$  is the acceleration due to the external tap and  $g = 9.8 \text{ m/s}^2$  is the gravitational acceleration):

$$K = \alpha\Gamma. \quad (5)$$

Taking  $\alpha=1$ , we will use  $\Gamma$  as a notation for this model parameter  $K$ .

(ii) The individual particles separated from the cluster by the single tap would immediately reassociate with other clusters in the system. For each particle the probability of reassociation,  $\gamma_j$ , with a cluster of size  $j$  was determined by

$$\gamma_j = \frac{n_j}{n_{\text{tot}}}, \quad (6)$$

where  $n_j$  is the number of clusters with  $j$  particles, and  $n_{\text{tot}}$  is the total number of clusters in the system. Expression (6) means that we consider an infinite granular medium, where all possible spatial combinations of clusters are realized, and we do not keep track of the mutual spatial positions of the clusters with respect to each other.

Our model has one dynamic parameter,  $\Gamma$ , and one fit parameter,  $v_1$ . Changes of  $v_1$  do not change the dynamics of compaction, but only change a scale of absolute values of the density  $\rho$ . A value of the parameter  $v_1$  was chosen so that the calculated steady-state density  $\rho$  at the applied acceleration  $\Gamma=7$  would match the experimental value of  $\rho$  at the same acceleration. The value  $v_1=0.9$  was used in our simulations.

Results of Monte Carlo simulations based on the described model and their discussion are given in the following section.

### III. RESULTS OF MONTE CARLO SIMULATIONS

#### A. Time evolution of the volume packing fraction

Figure 3 shows a typical Monte Carlo simulation of the density evolution for a system of 3000 particles at a fixed applied acceleration  $\Gamma=7$ . In close agreement with the results of experiments by Knight *et al.* [4] and Nowak *et al.* [22],  $\rho(t)$  increases logarithmically and eventually levels off at the longest times. Similar behavior was found for different values of  $\Gamma$  and could be consistently fitted to the form [4,22]

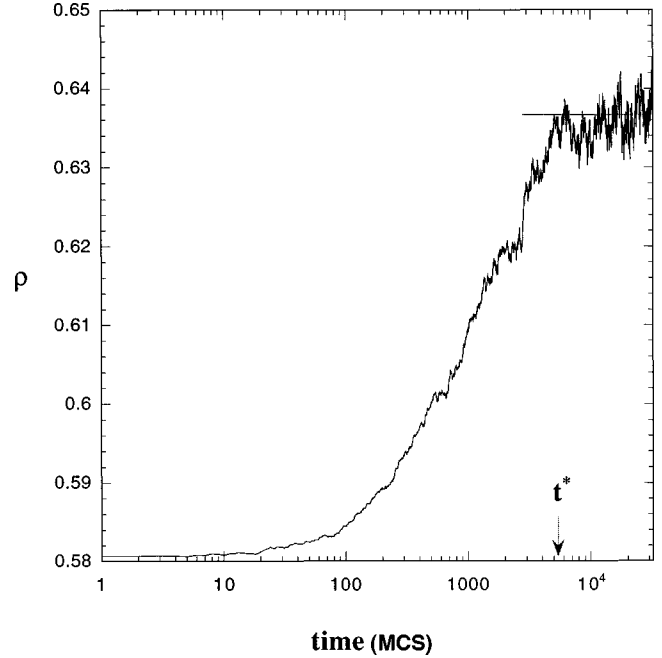


FIG. 3. Time evolution of the volume packing fraction,  $\rho$ , for a system of 3000 particles. The final steady-state density (dashed line) depends on the magnitude of applied external force, which is proportional to the dimensionless acceleration,  $\Gamma$ .

$$\rho(t, \Gamma) = \rho(\infty, \Gamma) - \frac{\rho(\infty, \Gamma) - \rho(0, \Gamma)}{1 + B \ln(1 + t/\tau)}, \quad (7)$$

where  $\rho(0, \Gamma)$  is the initial starting density (about 0.59 for our simulations) and  $\rho(\infty, \Gamma)$  the final, steady-state density after leveling off. The characteristic time of the leveling off,  $t^*$ , is a nonlinear function of the parameter  $\Gamma$  (Fig. 4). This functional dependence was fit with a function (8) shown in Fig. 4:

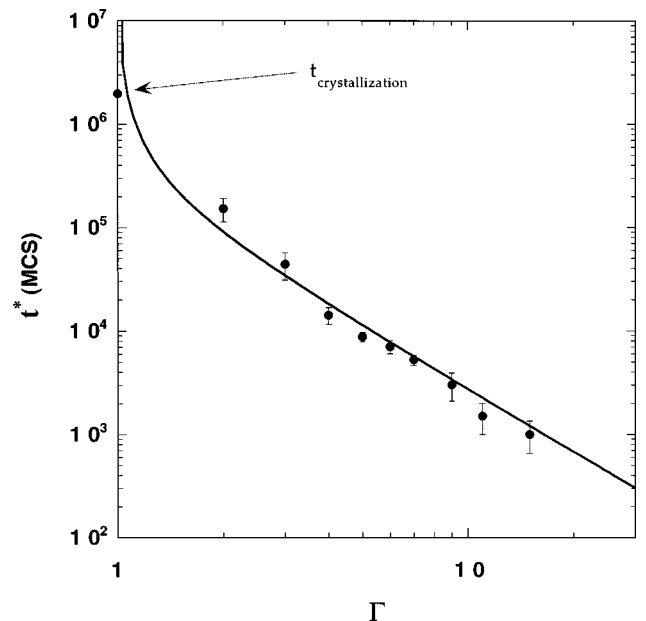


FIG. 4. Characteristic time of the leveling off,  $t^*$ , as a function of the parameter  $\Gamma$ . Solid line represents fit to the data with the function (8) given in the text.

$$t^* \sim \frac{1}{(\Gamma^2 - 1)}. \quad (8)$$

Simulations of the steady states extended for more than  $4 \times 10^7$  Monte Carlo steps (MCS) did not demonstrate noticeable drift of the average steady-state density.

It is interesting to note that smoothness of the  $\rho(t)$  curve (the amplitude of the density fluctuations) for  $t < t^*$  depends on the initial cluster distribution. The  $\rho(t)$  curve is a monotonously increasing function of time, when all the initial clusters are small ( $i \leq 3$ ) and, ideally, monodisperse. However, when the initial cluster distribution is randomized in a range  $2 \leq i \leq 20$ , the  $\rho(t)$  curve is not monotonous anymore, and the amplitude of the density fluctuations approaches the values observed in the experiments.

### B. Reversibility and irreversibility of granular compaction

Simulations closely reproduce the experimental results [20,22] for the density dependence on the history of how  $\Gamma$  was varied [Fig. 5(a)]: Starting from a low initial packing density at  $\Gamma = 0$ ,  $\rho$  increases with increasing  $\Gamma$  as voids are eliminated, and a system of loosely packed particles first undergoes irreversible compaction, corresponding to the lower branch of  $\rho(\Gamma)$ . For sufficiently large  $\Gamma$ , however,  $\rho$  eventually begins to slowly decrease since at higher accelerations void “annealing” through the clusters association competes with void creation during each tap due to the clusters fragmentation. If the cycle of increasing  $\Gamma$  is followed by a cycle of decreasing  $\Gamma$ , we find that  $\rho(\Gamma)$ , rather than following the original curve and decreasing back to its initial density, continues to increase until it reaches a maximum at  $\Gamma = 1$ . Subsequent changes of  $\Gamma$  (shown by squares) trace out a reversible, upper branch of the  $\rho(\Gamma)$  curve.

Our results show that because of exceedingly slow density relaxation with time, the irreversible behavior depends on the length of time  $\Delta t$  spent at each value of  $\Gamma$ . For the given number of taps per point,  $\Delta t$ , compaction behavior becomes reversible only after a characteristic acceleration  $\Gamma^*$  has been exceeded [ $\Gamma^* \approx 3$  for  $\Delta t \approx 3 \times 10^4$ , Fig. 5(a)]. It is also interesting to note that  $\Gamma$  and the average steady-state values of  $\rho$  are not necessarily independent. In fact, our model simply relates these two quantities to each other.

We also studied the dependence of the steady-state density ( $t \rightarrow \infty$ ) on  $\Gamma$  in the reversible regime [Fig. 5(b)]. For  $\Gamma \geq 2$ , the density values are close to the random packing limit and quantitatively agree with corresponding experimental density values [20]. However, for  $\Gamma = 1$  the entire system of beads transforms into a single cluster state with the maximal density  $0.74\rho_0$ . Growth of such single clusters with hexagonal packing, “crystallization,” was recently observed in experiments [23,24]. The characteristic time of crystallization,  $t_{\text{crystallization}}$ , starting with a random initial distribution of clusters, depends on the total number of beads in the system (Fig. 6), and scales as

$$t_{\text{crystallization}} \approx (0.7 \pm 0.3) N_{\text{tot}}^2. \quad (9)$$

No crystallization was observed in a system of 1000 particles after more than  $10^9$  Monte Carlo steps at  $\Gamma = 2$ .

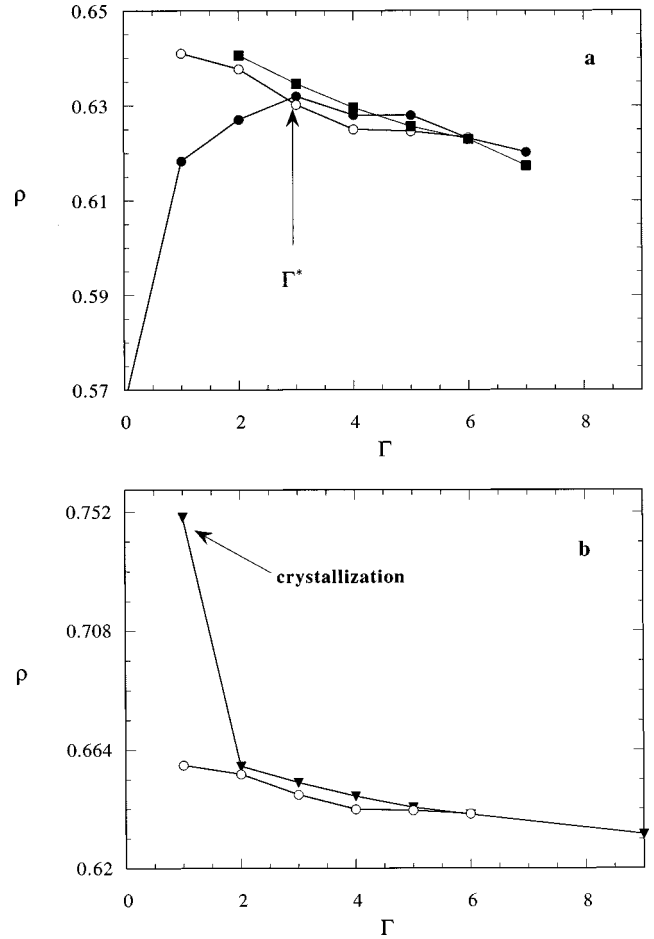


FIG. 5. (a) Density,  $\rho(\Gamma)$ , dependence on the history of how the vibration intensity  $\Gamma$  was applied for a system of 3000 particles. The closed symbols represent  $\rho(\Gamma)$  for a sequence of runs in which the vibration intensity was first incremented from  $\Gamma = 0$  up to  $\Gamma = 7$  with  $\Delta t \sim 3 \times 10^4$  taps at each value of  $\Gamma$ . The open symbols represent the density as the value of  $\Gamma$  was decreased back down to 1 (again with  $3 \times 10^4$  taps per point and after the achieved density was recorded). (b) The closed symbols represent dependence of the steady-state density  $\rho(\Gamma, t \rightarrow \infty)$  on  $\Gamma$  in the reversible regime. The open symbols represent the density as the value of  $\Gamma$  was decreased as in (a).

### C. Density fluctuations in the steady state

We have studied the density fluctuations around the average steady-state values in the reversible regime. Figure 7 shows the corresponding time record for a system of 3000 particles at  $\Gamma = 7$  (after previously applying  $10^5$  taps to reach the steady state). The power spectral density  $S_\rho(\omega)$  is plotted in Fig. 8. These spectra have Lorentzian shape and, for the entire range of accelerations, show two characteristic regimes: (i) a white-noise regime,  $S_\rho(f) \sim \omega^0$ , below some frequency value  $\omega^*$ , (ii)  $S_\rho(f) \sim \omega^{-2}$  above  $\omega^*$ . The values of the characteristic “corner” frequency  $\omega^*$  depend on the amplitude of  $\Gamma$  (Fig. 9) and can be fitted with a function:

$$\omega^* \sim \Gamma^2 \quad (10)$$

in quantitative agreement with corresponding experimental values [22].

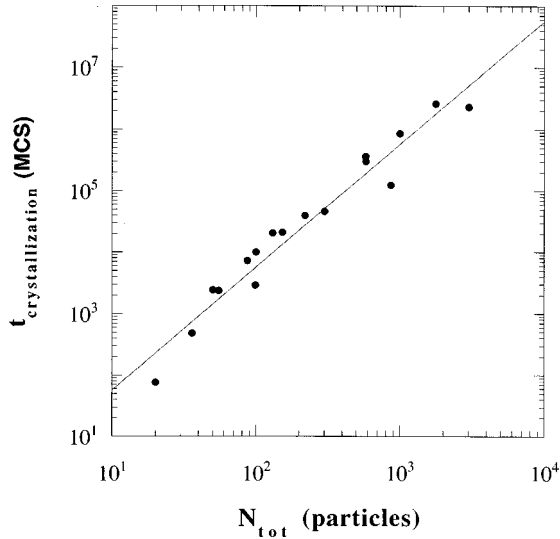


FIG. 6. Characteristic time of crystallization as a function of the total number of particles in the system. The straight line is a fit with quadratic function:  $t_{\text{crystallization}} \sim N_{\text{tot}}^2$  [Eq. (9)].

The ‘‘corner’’ frequency  $\omega^*$  can be related to the inverse of the characteristic time of the leveling off,  $1/t^*$  (Fig. 10). A linear fit to this plot yields the relationship

$$\omega^* = (0.56 \pm 0.06) \frac{2\pi}{t^*}. \quad (11)$$

This result means that the transition of the granular material, from an initial state with loose random packing to the steady state for  $G \geq 4$ , primarily depends on the cluster kinetics, but not on the initial cluster distribution. Thus, the kinetic data obtained from density fluctuations in steady state may be used to study the dynamics of irreversible compaction.

The power spectral density observed in the experiment [22] does not always have simple Lorentzian shape, and sometimes (near the bottom of a container with the granular material) deviates from  $\sim \omega^{-2}$  for frequencies above  $\omega^*$ . This deviation can be attributed to the gradual, one-by-one, reassociation of individual particles separated from a cluster [25]: at first, the individual particles are separated from a cluster during one tap and are ‘‘quenched’’ in such ‘‘separated’’ form; and then, only on following taps, these individual particles reassociate rapidly with surrounding clusters. This scenario can explain why in our simulations we do not

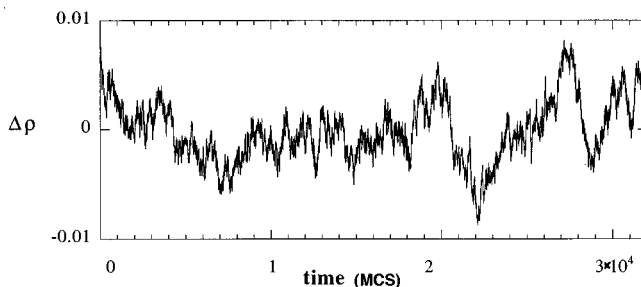


FIG. 7. Time trace of density fluctuations in the steady state:  $\Delta\rho$  is the difference between the instantaneous packing fraction and the steady-state density.

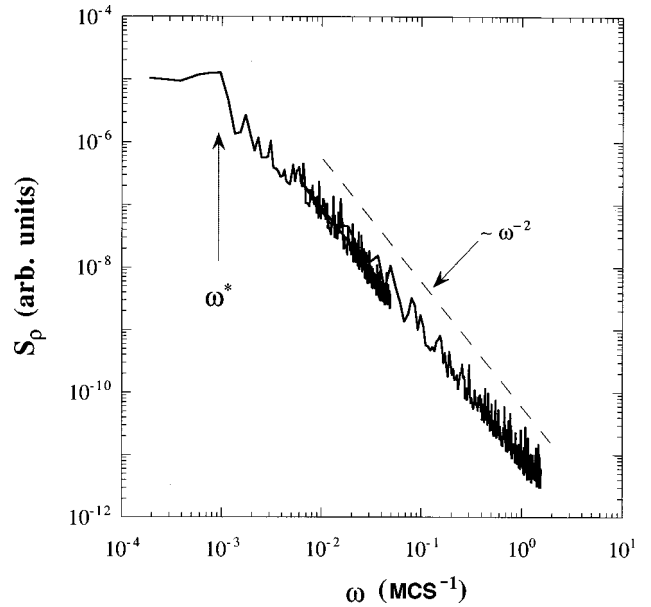


FIG. 8. Power spectrum corresponding to the extended record of the density fluctuations in Fig. 6. Dashed line,  $\sim \omega^{-2}$ , is given as a guide for the eyes. ‘‘Frequency,’’  $\omega$ , is measured in units of inverse Monte Carlo steps ( $\text{MCS}^{-1}$ ).

observe the deviation of the power spectral density from simple Lorentzian shape: it is because we assume that all individual particles separated from a cluster reassociate *immediately* (on the same tap) with surrounding clusters.

The cluster structure model accounts for the observed experimental amplitude of average density fluctuations, considerably higher than that expected from a statistical estimate:

$$\langle \Delta\rho^2 \rangle \sim N_{\text{tot}}^{-1}, \quad (12)$$

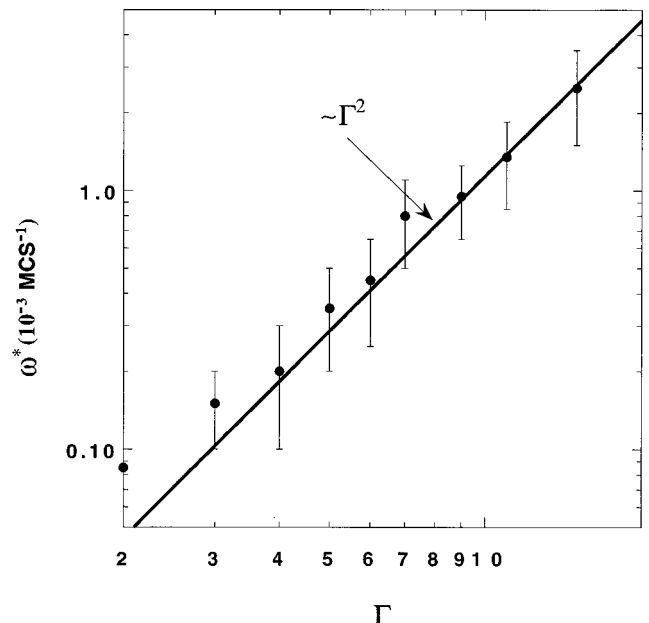


FIG. 9. The characteristic ‘‘corner’’ frequency,  $\omega^*$ , as a function of amplitude  $\Gamma$ . The functional form of the fit is  $\omega^* \sim \Gamma^2$  [Eq. (10)].

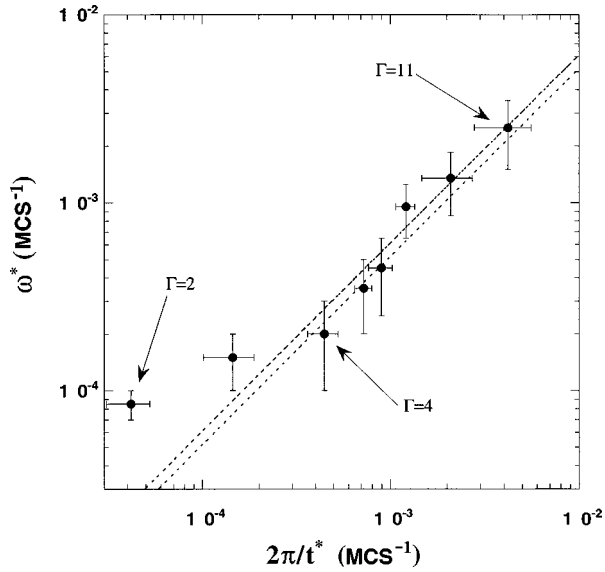


FIG. 10. Relationships between the corner frequency,  $\omega^*$ , and the inverse of the characteristic time of the leveling off,  $1/t^*$ . The fit function is  $\omega^* = (0.70 \pm 0.35) 2\pi/t^*$  [Eq. (11)].

where  $N_{\text{tot}}$  is the total number of particles in a system. Our model predicts instead that the average density fluctuations depend on the total number of clusters in a system (Fig. 11):

$$\langle \Delta \rho^2 \rangle \sim n_{\text{tot}}^{-1}, \quad (13)$$

where  $n_{\text{tot}}$  is the total number of clusters in a system. For a system of  $N_{\text{tot}} = 6000$  particles grouped into  $n_{\text{tot}} \approx 120$  clusters at  $\Gamma = 5$ , our model predicts  $\langle \Delta \rho^2 \rangle \approx 1.5 \times 10^{-5}$  (with the corresponding experimental value [22]  $\langle \Delta \rho^2 \rangle \approx 5 \times 10^{-5}$ ).

#### D. Steady-state cluster distributions

The simulations typically start with a random initial distribution of clusters with respect to the number of particles in

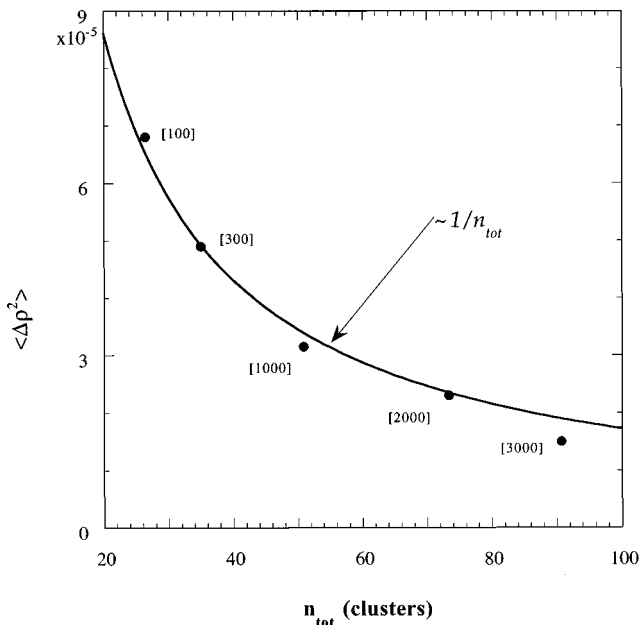


FIG. 11. The average density fluctuations at  $\Gamma = 7$  as a function of the total number of clusters in the system. The total number of particles in the system is given in the brackets.

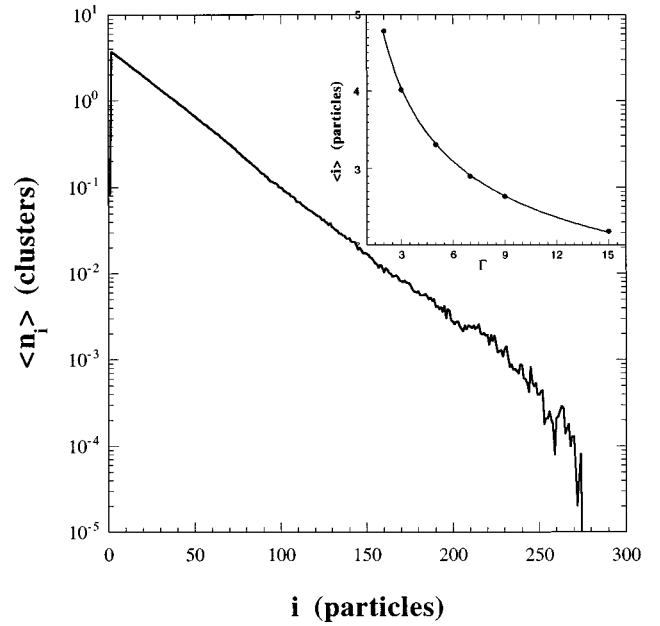


FIG. 12. A typical mean steady-state cluster distribution,  $n_i$ , for a system of 3000 particles at  $\Gamma = 7$ ; the distribution does not depend on initial conditions and has an exponential shape  $n_i = n_0 \Gamma^{(1-0.14i)}$  [Eq. (14)]. The inset shows the mean cluster size  $\langle i \rangle$  as a function of the acceleration  $\Gamma$  for the same system.

a cluster. The initial distribution evolves to a steady-state distribution. A mean steady-state distribution (Fig. 12) does not depend on initial conditions. The mean steady-state distribution has an exponential shape and for different values of  $\Gamma$  can be consistently described by a formula:

$$n_i = n_0 \Gamma^{(1-0.14i)}, \quad (14)$$

where  $n_i$  is the number of clusters with  $i$  particles in each,  $n_0$  is a normalizing constant depending only on the total number of particles in a system, and  $i \geq 2$ . These results suggest that our model could have a mean-field representation, similar to the Smoluchowski equation, that would describe the steady states and relaxation time from the initial to the steady state. Such mean-field theory would be useful for the study of more general classes of granular systems.

#### IV. DISCUSSION

The close agreement of our cluster model with experimental behavior raises the following question.

##### A. Why does this one-dimensional model describe so well the variety of dynamic effects in a three-dimensional system?

The agreement between experiment and simulations seems not just a matter of coincidence, but a generic result of the cluster approach. Actually, it is not the first time that a one-dimensional cluster model has described properties of two- and three-dimensional systems. Other examples can be found in, e.g., polymerization [26] and traffic flow on a multilane freeway [18,19]. The key feature of the cluster approach is that the dimensionality of a problem can be accounted for by the kinetics of individual clusters. In the case just studied this kinetics is described by formulas (4)–(6).

Thus, the comparison of these models' predictions with the experimental data suggests that the hypothetical granular clusters introduced in the model description are not just a convenient and efficient way of giving a mathematical description, but rather real entities, which determine the properties of the granular systems. The agreement of the model with the experimental behaviors implies a primary role of small strongly correlated regions (hexagonally packed clusters) on the properties of randomly packed material.

This, and the fact that the model gives direct control over the microdynamics of a granular system, could be used to extract microscopic properties of granular materials and constants of the elementary processes from the experimental data.

### B. This model as a tool to study the microdynamics of granular compaction

One can gain several insights into the microscopic properties of granular materials by varying the model parameters to fit the experimental data.

(i) How do clusters split? The cluster dynamics in Sec. II B supposes the fragmentation rate of clusters to be independent of cluster size. However, the fragmentation mechanism may depend on the cluster size. For example, one can imagine that the fragmentation may occur preferentially along a linear dimension of the cluster,

$$K \sim i^{1/3} \Gamma, \quad (15)$$

or on the entire cluster surface, and then

$$K \sim i^{2/3} \Gamma. \quad (16)$$

Our preliminary simulation results on steady-state fluctuations for these fragmentation scenarios indicate that the spectral shape ( $\sim \omega^{-2}$ ) is not affected when the fragmentation coefficient is varied from  $i^0$  [Eq. (5)] to either  $i^{1/3}$  [Eq. (15)] or  $i^{2/3}$  [Eq. (16)]. However, the "corner" frequency  $\omega^*$  and the average amplitude of fluctuation may change considerably. These effects may be relevant to those observed experimentally [20]: the integrated noise power near the top is smaller than the noise power closer to the bottom of a container filled by a granular material.

The fragmentation rate also depends on how much free space is available for individual beads to separate from the cluster. This leads to questions about cluster arrangement and voids sizes, as follows.

(ii) How do clusters arrange in a granular material? Our model has one fit parameter  $v_1$  mean void volume per one particle in a cluster. Its value may provide us with the answer to the question about clusters arrangement. This parameter was chosen to match a steady-state density at an applied acceleration  $\Gamma=7$  with its experimental value at the same acceleration.

(iii) We have assumed linear dependence of the rate of fragmentation on amplitude of external force and, thus, assumed linear dependence, Eq. (5), of the dynamic model parameter  $K$  and the dimensionless acceleration  $\Gamma$ . However, one can suggest different mechanisms for fragmentation as a function of the external force, e.g.,  $\sim \Gamma^2$  [in analogy with the different mechanisms of fragmentation as a function of size:

Eqs. (5), (15), and (16)]. We believe that it will be possible to study the relationship between  $K$  and  $\Gamma$  at different regimes of vibration by comparing experimental and theoretical results.

Many of the properties discussed above can be studied from measurements of density fluctuations in a steady state. This suggests measurements of the steady-state fluctuation as an effective experimental technique to study microdynamics of granular media. Result (9) indicates that the steady-state fluctuations can also be used for study of irreversible behavior of the granular media approaching the steady state.

Another interesting property to study is the crystallization. It will be very interesting to compare an experimental rate of the crystallization with the theoretical predictions of the rate.

## V. CONCLUSION

A microscopic one-dimensional model for compaction of a vibrated granular material has been proposed. In this model, the granular material undergoing vertical vibrations is considered as a system of randomly packed clusters. Each cluster in the system is supposed to have the maximum possible density achieved through hexagonal packing. Defects of packing are considered as mismatched placing of the hexagonally packed clusters. Vibrations cause fragmentation of clusters through separating of individual particles from clusters, and consequent reassociation of the individual particles with surrounding clusters.

The density state of the granular material is characterized by the distribution of clusters,  $n_j$ , with respect to the number of particles in the cluster,  $j$ . Compaction of a granular material is explained as an evolution of the cluster distribution. The steady-state cluster distribution, as a result of the detailed balance between fragmentation and association rates for each  $n_j$ , can be achieved when the intensity of external vibrations is fixed. The dependence of the value of the steady-state density on the intensity of the vibrations is explained as a shift in the equilibrium distribution of granular clusters due to the change of the fragmentation rate.

The irreversible behavior corresponds to the transition from a random initial cluster distribution to the steady-state cluster distribution, and the reversible behavior corresponds to the transition between the different steady-state cluster distributions.

For granular systems subjected to small external vibrations ( $\Gamma=1$ ), this model predicts the existence of a transition into the crystalline state (a single cluster with hexagonal packing).

The mechanism for cluster fragmentation suggested in the present paper describes spectral properties of the steady-state density fluctuations, such as a white-noise regime,  $\sim \omega^0$ , below the "corner" frequency  $\omega^*$ ;  $\sim \omega^{-2}$  regime above  $\omega^*$ ; and the values of the characteristic corner frequency  $\omega^*$ .

The results also suggest that this model, in combination with experiments on the steady-state density fluctuation, could be an effective experimental technique to study the microdynamics of granular media. It would be appropriate to emphasize a key feature of the model, namely, cluster approach: the view of granular media as systems with random packing of individual particles has been changed to considering the media as systems with random packing of clusters

of particles. The existence of small regions strongly correlated due to hexagonal packing can be a theoretical justification of such an approach.

It is important also to note computational usefulness and efficiency of the cluster approach, which allows us to subdivide the problem: (i) computation of kinetic properties of individual cluster, and (ii) computation of dynamics of granular media on the macroscopic scale. This subdivision, in principle, may allow for the incorporation of more elementary processes into theory, still preserving the efficiency of computations.

These first results of the simulations and their agreement with experiments demonstrate that this model, and the cluster approach in general, has a considerable potential for helping

to understand the behavior of granular materials. The predictive power of the proposed model will not fail to stimulate and facilitate the formulation of new experiments.

#### ACKNOWLEDGMENTS

The author thanks Riccardo Levi-Setti, L. P. Kadanoff, H. M. Jaeger, S. R. Nagel, and T. Witten at the University of Chicago, and E. R. Nowak at the University of Illinois at Urbana-Champaign for their stimulating discussions and suggestions. This work was supported through the MRSEC program by the National Science Foundation under Grant No. DMR 94-000379.

- 
- [1] B. J. Ennis, J. Green, and R. Davies, *Chem. Eng. Prog.* **90**, 32 (1994).
  - [2] For a recent review, see H. M. Jaeger, S. R. Nagel, and R. P. Behringer, *Rev. Mod. Phys.* **68**, 1259 (1996); *Granular Matter—An Interdisciplinary Approach*, edited by A. Metha (Springer-Verlag, New York, 1994); K. Rietema, *The Theory of Fine Powders* (Elsevier, London, 1991), and references cited therein.
  - [3] J. B. Knight, C. G. Fandrich, C. N. Lau, H. M. Jaeger, and S. R. Nagel, *Bull. Am. Phys. Soc.* **40**, 606 (1995).
  - [4] J. B. Knight, C. G. Fandrich, C. N. Lau, H. M. Jaeger, and S. R. Nagel, *Phys. Rev. E* **51**, 3957 (1995).
  - [5] S. J. Linz, *Phys. Rev. E* **54**, 2925 (1996).
  - [6] G. C. Barker and Anita Mehta, *Phys. Rev. A* **45**, 3435 (1992).
  - [7] G. C. Barker and A. Mehta, *Phys. Rev. E* **47**, 184 (1993).
  - [8] Eli Ben-Naim, J. B. Knight, and E. R. Nowak (unpublished).
  - [9] T. Boutreux and P. G. de Gennes (unpublished).
  - [10] A. Coniglio and H. J. Herrmann, *Physica A* **225**, 1 (1996); M. Nicodemi, A. Coniglio, and H. J. Herrmann, *J. Phys. A* **30**, L379 (1997).
  - [11] E. Caglioti, V. Loreto, H. J. Herrmann, and M. Nicodemi, *Phys. Rev. Lett.* **79**, 1575 (1997).
  - [12] M. A. Hopkins, and M. Y. Louge, *Phys. Fluids A* **3**, 47 (1991).
  - [13] I. Goldhirsch and G. Zanetti, *Phys. Rev. Lett.* **70**, 1619 (1993).
  - [14] Sean McNamara and W. R. Young, *Phys. Rev. E* **50**, R28 (1994).
  - [15] Y. Du, H. Li, and L. P. Kadanoff, *Phys. Rev. Lett.* **74**, 1268 (1995).
  - [16] T. Zhou and L. P. Kadanoff, *Phys. Rev. E* **54**, 623 (1996).
  - [17] E. Ben-Naim, P. L. Krapivsky, and S. Redner, *Phys. Rev. E* **50**, 822 (1994).
  - [18] K. L. Gavrilov, in *Proceedings of the 3rd International Conference on Powders and Grains*, edited by R. P. Behringer and J. T. Jenkins (A. A. Balkema, Rotterdam, Brookfield, 1997), p. 523.
  - [19] K. L. Gavrilov, *Phys. Rev. E* **56**, 4860 (1997).
  - [20] E. R. Nowak, J. B. Knight, M. Povinelli, H. M. Jaeger, and S. R. Nagel (unpublished).
  - [21] E. R. Nowak, M. Povinelli, H. M. Jaeger, S. R. Nagel, J. B. Knight, and Eli Ben-Naim, in *Proceedings of the 3rd International Conference on Powders and Grains*, edited by R. P. Behringer and J. T. Jenkins (A. A. Balkema, Rotterdam, Brookfield, 1997), p. 377.
  - [22] E. R. Nowak, J. B. Knight, Eli Ben-Naim, H. M. Jaeger, and S. R. Nagel, *Phys. Rev. E* **57**, 1971 (1998).
  - [23] L. Vanel, A. D. Rosato, and R. N. Dave, in *Proceedings of the 3rd International Conference on Powders and Grains*, edited by R. P. Behringer and J. T. Jenkins (A. A. Balkema, Rotterdam, Brookfield, 1997), p. 385.
  - [24] H. M. Jaeger and M. Medved (personal communications).
  - [25] A. J. Kolan, E. R. Nowak, and A. V. Tkachenko (unpublished).
  - [26] P. Meakin, *Rep. Prog. Phys.* **55**, 157 (1992).